Prolonged or perpetual growth of replacement teeth in the rock hyrax

Timothy D. Smith[1,*], Laura Bento Da Costa[2], Sarah E. Downing[3], Christopher J. Bonar[4], Anne M. Burrows[3], Kristen A. Prufrock[5], Christopher J. Vinyard[6], Valerie B. DeLeon[2]

1 Department of Health and Rehabilitation Sciences, Slippery Rock University, Slippery Rock, PA

2 Department of Anthropology, University of Florida, Gainesville, FLA

3 Department of Physical Therapy, Duquesne University

4 Franklin Park Zoo, One Franklin Park Road, Boston, MA

5 Department of Neuroscience, Washington University in St. Louis

6 Biomedical Sciences, Heritage College of Osteopathic Medicine, Ohio University, Athens, Ohio,

Funding by NSF grants BCS-2235657, BCS-2235578, BCS-2235665

* Corresponding author:

Tim D. Smith, Ph.D., School of Physical Therapy, Slippery Rock University, Slippery Rock PA, 16057

phone: 724-738-2885; fax: 724-738-2113

e-mail: timothy.smith@sru.edu

This is the peer reviewed version of the following article: Smith TD, Bento Da Costa L, Downing SE, Bonar CJ, Burrows AM, Prufrock KA, Vinyard CJ, DeLeon VB. Prolonged or perpetual growth of replacement teeth in the rock hyrax. The Anatomical Record. Early view, 2024 Dec 31, which has been published in final form at https://doi.org/10.1002/ar.25625. This article may be used for non-commercial purposes in accordance with Wiley Terms and Conditions for Use of Self-Archived Versions.

ABSTRACT

Tusks are ever-growing teeth present in mammals of the clade Paenungulata. Unlike the perpetually growing incisors of rodents, tusks are not used in mastication, and in at least some paenungulatans, the tusk is composed of dentin alone in adults. Few studies have provided tissue-level information on tusks of adult paenungulatans with embedding techniques that identify epithelial and other soft tissues. In order to examine the mineralized tissues as well as the cells that form teeth, we studied a single, subadult rock hyrax (*Procavia capensis*) using microCT and paraffin histology with traditional staining as well as RUNX2 immunohistochemistry, and compared its teeth to scans of adult hyraxes. Three-dimensional reconstructions from microCT volumes revealed that the tusk of this specimen is the only fully erupted replacement tooth, the first adult premolar (P1) is starting to erupt, and the first permanent molar (M1) is fully erupted, whereas all other replacement teeth and M2 remain in crypts. The tusk has a thin layer of enamel on its dorsal side; this is confirmed by histology. All deciduous premolars still possess roots that are in the process of resorption. Amelogenesis has progressed to maturation or nearly so in P1 to P3. Notable histological characteristics of replacement premolars include the lack of a stellate reticulum in all except P4, and expression of RUNX2 in ameloblasts, a marker which is expressed by ameloblasts at all stages of amelogenesis. P4 exhibits the “picket-fence” appearance typical of ameloblasts still secreting protein. The pulp chambers of replacement premolars are relatively large compared to adults. This may indicate that the lengthy time in crypts is important for dentin production. The results confirm that the hyrax has thin enamel on tusks, supporting the hypothesis that enamel is of limited importance for non-feeding behaviors.

1 INTRODUCTION

Mammals with continuously growing teeth present exceptional tissue level traits that distinguish these teeth from primary or secondary teeth that erupt for prolonged use, but cease growth once erupted. Notably, continuously growing incisors of rodents retain a layer of ameloblasts to continuously secrete enamel (Coady et al., 1967; Wyss et al., 2016), whereas these cells undergo apoptosis in other tooth germs (Lee et al., 2012). Tusks are ever-growing teeth that attain an extraoral position (Nasoori, 2020). Constant abrasion of tusks is another feature, complementing their constant growth (Nasoori, 2020); in this respect rodent incisors are no different, since with the lack of a sufficiently abrasive diet these teeth "overgrow" (Legendre, 2002).

There are distinctions between tusks and rodent incisors beside the extraoral position of the former. For example, elephant tusks possess a limited extent of enamel, confined to the cusp tip. According to Virág (2012), this enamel wears away with years after eruption of the tusk (i.e., the replacement incisor). Whether this is an unusual feature typifying adult elephants or perhaps all of the clade Paenungulata (Proboscidea, Sirenia and Hyracoidea) remains unclear. In either case, lack of enamel is unusual for mammals. It should also be emphasized that in the earliest tusk-bearing synapsids, enamel is thought to have been present on these enlarged teeth (Whitney et al., 2021). This makes absence of enamel more striking. Another example of absent enamel (though still in debate) may be in the teeth of vampire bats (Hermanson and Carter, 2020). A commonality of vampire bat teeth and tusks is that they are not important for all aspects of feeding (e.g., mastication). In vampire bats, sharp incisors are specifically used to pierce skin, not mastication (Fenton, 1992). Tusks are employed in defensive behavior and to manipulate structures or objects such as vegetation (Nanori, 2020).

Testing whether other paenungulatans lack enamel in tusks is best explored as a tissue level question. For example, histological or radiographic methods offer a means to identify enamel. Further, a question remains even if enamel forms and wears away permanently: are ameloblasts still present in the dental crypts of the tusk? A major impediment to the study of tusks is the size of tusked mammals. Elephants, the largest living land mammals, as well as several marine mammals (narwhals, walruses) are inconveniently large for many CT scanners and are especially challenging for histological methods. Even smaller tusked mammals such as babirusas or hyraxes are less than ideal for histological study because of their body size. Due to these limitations, our knowledge of replacement tooth and molar ontogeny in tusked mammals is far less compared to a reasonably robust number of studies on deciduous incisors that precede tusks (e.g., Woodward, 1892; Adloff, 1903; Luckett, 1993; Gomes Rodrigues et al., 2020; McKay et al.,

2022). To our knowledge, histological studies of tusks are almost non-existent, excluding work on dry skeletal material (e.g., Virág 2012).

Whereas tissue level observations are rare, there have been some studies establishing postnatal dental eruption patterns in tusked mammals, including elephants (Roth and Shoshani, 1988). Smaller extant relative of elephants, the hyraxes, have been better studied, perhaps due to their smaller size. Rock hyraxes (*Procavia capensis*), for example, range from 3 to 4 kg (according to Horne and Loomis 2007), with average weights of 3.6 kg for females and 4 kg for males (Olds and Shoshani, 1982). Their continuously growing upper incisors are not used in feeding, and are proposed to have their greatest importance in defense of the entrance to their rocky burrow (Sale, 1966). Feeding is accomplished with sharp-edged premolars and molars; they are considered efficient feeders (Sale, 1966). They possess numerous molariform teeth whose eruption has been well studied (Fairell, 1980; Steyn and Hanks, 1983; Asher and Lehmann, 2008). Among afrotherians, hyraxes (as well as elephants) are said to be notable for late eruption of replacement teeth (Asher and Lehmann, 2008). Steyn and Hanks (1983, p 247) stated that in *Procavia* "all teeth are fully erupted and in wear by five years of age" which is half the suggested lifespan for this species. Fairell (1980) reported a slightly faster schedule of full permanent tooth eruption by 36 months, but M3 wear is delayed until later. Regarding the tusk, Fairell (1980) notes that it cuts the gums at eight months of age, and matches the length of the deciduous incisor at ten months of age.

Because of their relatively small body size, rock hyraxes are of manageable size for traditional histological methods. In the present study, we use a single, cadaveric subadult rock hyrax (*Procavia capensis*) that possesses mixed dentition to address the lack of detailed histological data. Our general focus is on the odontogenic tissues (e.g., inner enamel epithelium, odontoblasts, dental follicles). By examining these odontogenic tissues, we seek to understand crown formation in tusks, teeth that are perpetually erupting, as well as replacement premolars, teeth that are relatively late to erupt. In particular, we test the hypothesis that hyrax tusks lack enamel production and perhaps enamel-producing epithelium postnatally, as appears to be the case in at least some of their living relatives, notably elephants.

2 MATERIALS AND METHODS

2.1 Sample and CT methods

One rock hyrax (*Procavia capensis*) was studied. The specimen (# M90628), acquired from the Cleveland Metroparks Zoo after dying in captivity, was male and 11

months, 22 days of age at death. At this age, the hyrax was sexually immature (Olds and Shoshani,1982). The skull is also not likely fully grown since it was undersized compared to published findings on adults. For example, bi-zygomatic breadth was 47.40 mm, compared to 51.8 to 62.3 mm in adults and the length of maxillary toothrow was 32.88 mm, compared to 39.0 to 42.7 mm in adults (adult measurements from Olds and Shoshani,1982). During necropsy, the head was carefully dissected to remove the intact snout region, which was then immersed in 10% formalin, with no prior freezing. Use of these tissues was reviewed and approved by the IACUC committee at Slippery Rock University.

First, the head of the specimen was μ-CT scanned at Northeast Ohio Medical University (NEOMED) using the Scanco vivaCT scanner (scan parameters: 70 kVp; 114 μA). The volumes were reconstructed using 35 μm cubic voxels with 8-bit grayscale values ranging from 0 to 255 (see DeLeon & Smith, 2014). Three-dimensional digital reconstruction from the μ-CT volume for the specimen M90628 were rendered using the 3D Slicer software, in full resolution (0.0035*0.0035*0.0035 mm cubic voxels). The same software has been used for the measurements of the bi-zygomatic breadth and the length of the maxillary toothrow (markup module).

Analysis of grayscale levels of the crowns was accomplished for all teeth by scanning through serial microCT slices using ImageJ software (NIH). Peak gray scale levels for each tooth were noted based on slice number and position on the crown (buccal, lingual, or occlusal surface). Location of the slice levels is indicated on 3D models of the tusk is shown in Figure S1. MicroCT methods do not aid in tissue identification in such a way that predentin can be distinguished from dentin, or that the dentoenamel junction can be specifically indicated when enamel is not fully mineralized. However, we sought to approximate “presumptive enamel” whenever a band distinctly higher radio-opaque tissue was observed near the crown surfaces. This band was then measured using ImageJ in order to compare presumptive enamel depth in different teeth (e.g., Figs. S2, S3). Using the same line that was drawn to measure presumptive enamel thickness, we used the “Plot Profile” function (under the “Analyze” menu in ImageJ) to obtain the full range of gray levels within the band of presumptive enamel. The range of gray levels in dentin was obtained by tracing the deeper mineralized crown tissue using a free selection tool in ImageJ. When tracing the pulp cavity and innermost part of the enamel were carefully avoided (Fig. S2).

The grayscale levels of the presumptive enamel in microCT scan slices was converted to hydroxyapatite (HA) density with a linear conversion of grayscale values. Each grayscale value was converted to an HA density using a known calibration standard of HA density (R2 = 0.99) provided by the scanner manufacturer (Scanco). Using this regression equation ($y = 6.9269x - 222.8126$), HA density reaches 0 at approximately a gray level of 32.

We assume this level approximately indicates the threshold between predentin and the least mineralized dentin. Establishing peaks and ranges of hydroxyapatite density in each tooth allowed us to infer how the pace of mineralization differed across the dental arcade in rostrocaudal space.

For a comparison, two scans of adult rock hyraxes were visualized using Amira. These specimens (both from the Cambridge University Museum of Zoology, #s H4981F and H5101A) were previously scanned by Asher et al. (2017) and were available through MorphoSource. Here, we used the specimens to qualitatively describe the difference in dentin thickness of our subadult specimen compared to adults.

2.2 Histological processing and sectioning

After scanning, the specimen was dissected to aid infiltration of paraffin, producing a "hemisnout," including the palate, for histology. The tissue was decalcified in a sodium-citrate formic acid solution. After decalcification the head was briefly re-fixed in formalin, then dehydrated in graded ethanols, cleared in xylene, and paraffin-embedded in a vacuum oven (more details in DeLeon & Smith, 2014). The paraffin block was mounted on a wooden post and serially sectioned at 12 µm, then alternative sections were stained with hematoxylin-eosin, or Gomori trichrome procedures. Serial sections were accomplished throughout all levels containing the tusk and premolars. M1 and M2 were not histologically sectioned, but were examined radiographically.

2.3 Immunohistochemistry

To further assess the soft tissues surrounding the tooth germs or replacement premolars and the tusk, we employed RUNX2 immunohistochemistry. This marker is expressed in ameloblasts, and in differentiating and mature osteoblasts and cementoblasts (Diep et al., 2009; Liu et al., 2019, and see Camilleri et al., 2006), thus allowing interpretation of enamel production, and possibly follicle-derived cells that deposit alveolar bone and cementin. To prepare tissue slides for immunohistochemistry, deparaffinized and rehydrated sections were subject to heat induced epitope retrieval (HEIR) in citrate buffer, pH 6.0 at 60°C overnight. Slides were allowed to cool in the buffer, then rinsed 3x with tris-buffered saline (TBS). Tissue sections were blocked with 10% goat serum in TBS for 2 hours at room temperature, prior to incubation with a RUNX2-specific primary antibody (Santa Cruz, sc-390715, 1:50 in TBS + 1% BSA) overnight at 4°C. Tissue sections were then rinsed in TBS, and endogenous peroxidase activity was blocked by treatment with 0.3% hydrogen peroxide in TBS for 15 minutes. Following this, tissue

sections were rinsed 3x in TBS, prior to secondary antibody (Vector Laboratories, BA-9200, 1:200 in TBS + 1% BSA) incubation for 30 minutes at room temperature. Tissue sections were then rinsed in TBS, then incubated with VECTASTAIN® Elite® ABC-HRP reagent (Vector Laboratories, PK-6105) for 30 minutes at room temperature. Following this, tissue sections were rinsed in TBS then incubated with DAB substrate (Vector Laboratories, SK-4100) until sufficient color had developed. Slides were subsequently dehydrated, cleared, and coverslipped for microscope analysis.

3 RESULTS

3.1 MicroCT observations

Three-dimensional reconstruction of the skull and superior dental rows revealed one tusk (incisor, I1), four decidual premolars (dp1-dp4), four permanent (replacement) premolars into crypts (P1-P4) and two permanent molars (M1-M2) (Dental formula of the superior row = 1.0.4.2). The decidual canine is absent, probably because of the eruption of the P1 at this late advanced development stage, and the deciduous dI2 as well. Compared to the dental formula of adults (1.0.4.3) (Olds and Shoshani, 1982; Asher et al., 2017), the difference is the absence of the M3, not developed yet at this age (Asher et al., 2017). The tusks and the first decidual premolar dp1 are separated by a diastema. The crypts of the tusks extend above and overlap the levels of dp1/P1 to dp2/P2, ending on the rostral border of the dp3/P3 (Fig. 1). The tusks possess a triangular cross-section, and their dorsal side is recovered by a thin enamel layer (Fig. 1a).

The decidual premolars dp1-dp4 are fully erupted. The first decidual premolar dp1 possesses three circular roots, dp2 and dp3 five (a thin supplementary one in the middle of the two caudal roots) and dp4 shows four roots. All the decidual premolars show a resorption of their roots (Fig. 1b, e), at a higher rate for the lingual roots compared to the buccal ones. The roots of dp2 are circular in cross-section, as the buccal roots of dp3 and dp4, while the lingual roots of dp2, dp3 and dp4 are more oval and rostro-caudally compressed. The fifth caudo-central root of dp2 and dp3 is round. The first permanent premolar P1 starts its eruption, showing a rostral circular root and a caudal oval one (extending on the entire width of the P1). The crowns of the replacement premolars (P1-P4) are totally formed, while the roots are partially developed (two roots for P1, four for P2 and P3), except for P4 for which the root development did not start. The two lingual roots of P2 are still fused. The permanent P2, P3 and P4 are present deep in enclosed crypts.

Concerning the molar region, M1 is fully erupted, with its roots almost fully developed (apical closure almost fully formed). Four principal roots are present, with a fifth round and

thinner one positioned between the two caudal roots. The M2 is present deep in a partially enclosed crypt open rostro-ventrally. The roots are not formed yet, the dental base partially developed. There is no evidence of M3 formation, with maxillary bone fully ossified and no obvious space available for the eventual development of an M3 crypt (Fig.1c-e).

3.2 Histological findings and hydroxyapatite density

The tusk (I1) overlaps the first two premolars until the caudal side of the dp2/P2, the crypt terminating rostral to the level of P3/dp3 (Figs.1-3). The tusk is housed in the premaxillary bone (Fig. 2) which diminishes to a cylindrical, thin-walled shell more caudally (e.g., shown in Figs. 3a,b, g). The internal enamel epithelium is observed along most of the rostrocaudal length of the tusk (Fig. 3c). A notable increase in thickness of dentin occurs from caudal to rostral (Figs. 3-d-f), but enamel is only seen caudally in histology, where it is a thick, densely stained fragment (Fig. 3f).

When viewing the undecalcified head (via microCT), the enamel is detectable rostrally and at mid-length levels of the tusk as a very thin layer that is visible on the buccal side of the tusk (insets of Figs. 3d and 3e). At more caudal levels the enamel is not detectable, suggesting it is a similar density of hydroxyapatite density is dentin. Enamel thickness on the tusk appears to range from 0 to 170 micrometers. Voxel resolution was only 35 microns, so our ability to accurately measure enamel thickness in serial sections is limited. Nevertheless, plot profiles using ImageJ can shed some light (see section 3.3).

Comparison to adult specimens scanned by Asher et al. (2017) revealed relatively smaller pulp cavities exist in adult replacement premolars (Fig. 1).

The P1 is surrounded around the sides of the crown by mostly high columnar inner enamel epithelium (IEE), whereas the occlusal surface is covered with reduced enamel epithelium (Fig. 2c). The IEE diminishes in height near the cervical part of the crown (Figs. 2d, e). No trace of a stellate reticulum is observed, and there are no discrete cellular layers peripheral to the IEE, rather a mix of cells and blood vessels, suggesting the stratum intermedium and outer enamel epithelium have transformed to the papillary layer. The dentin of P1 is surrounded by a large enamel space (an artifactual gap created due to enamel decalcification, and breakdown); its dentin stains deeply red with Gomori trichrome stain, as contrasted with bright green predentin (Fig. 2f).

The second replacement premolar is surrounded by a thick enamel space. Dentin is also thick and densely stained with trichrome, although only the lingual side and the occlusal surface stains red, the remainder of crown dentin stains deeply green (Fig. 3b, h). The IEE is entirely similar to P1 (Fig. 3i), and no stellate reticulum is observed.

The P3 was mostly damaged in preparation and the IEE could not be studied in detail.

The last replacement premolar is distinct from the more rostral premolars in dentin and enamel histology, and in the IEE morphology. The enamel of P4 is radiographically indistinct, except near the cusp tip (Fig.4a). In histological sections, enamel is more intact than in P1, P2, and P3. It is especially intact and densely stained near the cervix of the crown (Figs. 4b, c), and small patches of enamel survived sectioning at the occlusal surface. The IEE-enamel interface exhibits the "picket-fence" appearance indicative of the presence of Tomes' processes (Fig. 4d). The IEE at the occlusal surface possesses a low columnar morphology (although at this site the IEE is freed from adjacent connective tissue, and therefore might have been subject to relatively more shrinkage during processing). Stellate reticulum is detectable along the buccal and lingual sides of the crown near the cusp tips, where it is observed only in patches due to artifactual damage.

The deciduous premolars all stain densely with trichrome, displaying regions with affinity for either red or green dyes (e.g., Figs. 2b, 3b).

3.3 Immunohistochemical results

The tissues surrounding the tusk and first replacement premolar (P1) have specific tissues and cells that are reactive to the RUNX2 antibody (Fig. 5). P1 has RUNX2+ cells visible near the root of the tooth (Fig. 5b) as well as the cervical region of the tooth (Fig. 5c). Along the crown, the IEE had numerous RUNX2+ ameloblasts, but no RUNX2 +cells were found in adjacent connective tissues (Fig. 5d), in contrast to the root. The tissue surrounding the enamel-bearing surface of the tusk is similar to that described along the crown of P1: The IEE is RUNX2+ whereas no RUNX2+ cells are seen in adjacent connective tissues (Fig. 5e). Negative controls reveal that with omission of the primary antibody there is no discernable non-specific background staining.

3.4 Ranges of hydroxyapatite density of presumptive enamel and dentin

Overall, peak hydroxyapatite (HA) density of the tusk is observed in rostral-most 40% of rostrocaudal space occupied by the tusk. Nearest to the cusp tip, peak density is 789 mg HA/cm^3 (site 1, Table 1) whereas at the 40th percentile of rostrocaudal tusk length, peak density is 689 mg HA/cm^3 (site 3, Table 1). Between these two levels, the highest density is 789 mg HA/cm^3 (site 2, Table 1). Caudal to site 3, peak densities gradually decline; by the 75th percentile, peak HA density is barely more than ~ 500 mg HA/cm^3. This

is notable because areas of presumptive dentin (Figs. S2 and S3) are </= to this same density. Thus, we surmise that the enamel at the 75th percentile (as shown in Fig. 3f, inset; also see site 4, Table 1) and more caudally is only as mineralized to the same extent as the densest dentin at this point in ontogeny.

The first three sites of the tusk described above show distinct bands of enamel, and measured at ~ 170, 170, and 100 µm in thickness, respectively. Peak densities change in their position across space. Peaks are observed on the dorsal side of the cusp tip most rostrally. Moving caudally, peak density shifts to the buccal side for the rest to the rostral half of the cusp. But after the rostral half, the enamel becomes less and less distinct from underlying dentin, even though its presence is known based on histology (see above). By the 75th percentile, the densest cusp tissue, presumably immature enamel, shifts back to the dorsal side of the cusp (Fig. S2).

The site of peak HA density of P1 is on the buccal side of the cusp. Here, the highly radio-opaque band of presumptive enamel is ~ 240 thick with a peak density of 955 mg HA/cm^3 (Fig. S3).

The site of peak HA density of P2 is on the buccal side of the cusp. Here, a highly radio-opaque band of presumptive enamel is ~ 310 µm thick with a peak density of 1017 mg HA/cm^3 (Fig. S3).

Peak HA density of P3 is observed on the occlusal side of the crown. Here, a distinct radio-opaque band is present (Fig. S3). This presumptive enamel is ~ 330 µm thick with a peak density of 1024 mg HA/cm^3. The site of highest density of enamel on the buccal side of P3 is ~ 280 µm thick with a peak density of 982 mg HA/cm^3 (Fig. S4).

Peak enamel density of P4 is observed on the buccal side of the P4 crown, and a distinct radio-opaque band is only present near the cusp tip (Fig. S3). The presumptive enamel is ~ 240 µm thick and ranges 892 mg HA/cm^3.

For dp1, dp2, dp3, and dp4, peak HA densities are at 996, 1073, 1045, and 1059 mg HA/cm^3, respectively.

M1 has a radiographically distinct band of presumptive enamel. There are two sites of peak density (both at 1128 mg HA/cm^3), one found buccally and the other at a more distal occlusal position. At both these sites, there is a distinct radio-opaque band of presumptive enamel (Fig. S5). These enamel bands are ~ 350 µm and ~ 360 µm thick, respectively, at buccal and occlusal sites.

M2 has a radiographically distinct band of presumptive enamel. Peak density is observed buccally. Here, there is a distinct radio-opaque band of presumptive enamel (Fig. S6). This band is ~ 345 µm thick with a peak density of 1024 mg HA/cm^3.

Qualitatively, dentin is thickest rostrally in the tusk (Fig. S2). It is also thicker in P 1 to 3 than in P4 (Fig. S3). Dentin is thicker in the mesial than the distal parts of M1 (Fig. S5), and thicker in M1 than M2 (Fig. S6). The range of HA density of dentin in permanent teeth may be described as lowest in the tusk (352 to 657 mg HA/cm^3 across the length of the cusp; Table 1), intermediate among all replacement premolars (465 to 712 mg HA/cm^3), and highest in (428 to 823 mg HA/cm^3). In the deciduous premolars, dentin ranges are broadly similar among the four teeth, ranging from 338 to 775 mg HA/cm^3.

4 DISCUSSION

Tusks are ever-growing teeth present in mammals of the clade Paenungulata (elephants, sirenians, hyraxes). Histology of developing teeth in hyraxes and elephants has been done previously, but only in prenatal samples (Woodward, 1892; Adloff, 1903; Raubenheimer, 2000). The subadult hyrax studied here offered a rare opportunity to examine mineralized tissues of teeth in a subadult animal with mixed dentition, but also soft tissue characteristics of tissue surrounding the tusk and replacement tooth germs. Our findings refute the hypothesis that all paenungulatans lack tusk enamel; further work must be done to confirm prior suggestions of complete enamel loss in elephant tusks. However, the finding of thin enamel in hyraxes nonetheless is consistent with to hypothesis that enamel is of limited importance for non-feeding functions.

In our study we also encountered a subadult jaw that is packed with exceedingly large developing replacement teeth. Below, we will discuss unusual microanatomical features that begin to explain strategies for growth of teeth that perpetually replace dentin and enamel, or teeth with a prolonged pre-eruption phase that may serve to maximize thickness of dentin and enamel.

4.1 Enamel and dentin in the subadult hyrax

Unlike the perpetually growing incisors of rodents, tusks are not used in mastication, and in at least some paenungulatans, the tusk is composed of dentin alone in adults (Virág, 2012). Here we find that postnatally, the tusk has enamel on its dorsal surface. The enamel is exceedingly thin (relative to dentin) compared to premolars and molars of the subadult, and continues to be present as a thin layer in adults. Since CT

scans cannot always detect dentin-enamel junctions with accuracy, especially in subdadults, it is important to note the presence of a thin enamel layer is confirmed by histology (Fig. 3f). Combined with the lack of enamel in adult elephants (Virág, 2012), this implies that enamel may be of limited importance for tusks, and perhaps for non-feeding behaviors generally.

Findings on crowns of premolars and molars reveal a number of trends in mineral density and development. In the rock hyrax studied by histology, mixed dentition afforded us an opportunity to examine tooth HA density across rostrocaudal space of the upper jaw. For both primary and secondary teeth, HA density increased in more caudally positioned teeth (excluding P4, which had less mature enamel overall than other premolars), and was typically higher on the buccal side in all teeth. M1 represented the case of thickest and densest enamel. Generally, this agrees with findings on primates, in which mineral density of enamel is higher in parts of the crown with the thickest enamel, a possible dietary adaptation (Towle et al., 2023).

Some ontogenetic aspects of enamel and dentin of replacement teeth can be surmised in the rock hyrax. It is important to point to common artifacts of paraffin histology. Since paraffin histology requires decalcification of specimens prior to histology, all that remains of calcified tissue is extracellular matrix (e.g., collagen and ground substance). However, during late enamel maturation ground substance molecules are resorbed, leaving mainly inorganic content (Nanci, 2003). Thus, mature enamel is "dissolved" and leaves little if any remnants during sectioning; hence, the enamel space. Immature enamel is less mineralized and still contains the organic connective tissue content (ground substance) that holds it together during paraffin sectioning (Nanci, 2003). With this in mind P1 to P3 show very mature enamel, typical of teeth at a pre-eruptive state (although enamel maturations for P2 and P3 may still be occurring, see below). P4, completely enclosed in its crypt is at an earlier stage of amelogenesis, and presents with continuous enamel.

Judging by the size of the pulp cavity, dentin in all replacement teeth in the subadult is proportionately less thick than in the same teeth of adult specimens previously studied by Asher et al. (2017). Dentin is continuously produced throughout postnatal life, unlike enamel. If hyrax replacement tooth eruption is relatively delayed compared to most mammals, as suggested by Asher and Lehmann (2008), we suggest that prolonged time in the crypt may allow increases in dentin thickness prior to eruption, in particular. For context, the specimen examined here is still at a relatively early stage of dental eruption. A 24 month-old hyrax would have an erupted M2 with "slight signs" of wearing; After 36 months all teeth except M3 erupted (Fairell, 1980).

4.2 Soft tissues surrounding the tusk and replacement teeth

Histology confirms the presence of an IEE surrounding the dorsal side of the tusk in the hyrax. The gomphosis is well developed, an ancient characteristic of tusks (Whitney et al., 2021). Similar histological work, though it would be markedly more difficult, has not been done on postnatal elephants to date. If enamel production ceases, as suggested by macroscopic evidence (Virág, 2012), the IEE may degenerate postnatally in elephants.

Normally, RUNX2 is abundantly expressed in the IEE of postnatal rodents (though not in every ameloblast). The marker is expressed by ameloblasts at all stages of amelogenesis (Liu et al., 2019); RUNX2, among other transcription factors, appears to be essential for amelogenesis. Thus, expression in hyrax tusks, which do possess enamel, seems unsurprising. However, its expression in the more rostral premolars, even P1, may indicate that some final events of amelogenesis (mainly resorption of organic matrix) are still occurring in these teeth, most of which are pre-eruptive. We make these interpretations cautiously, because only one specimen is studied here.

RUNX2 is also expressed in some cells in the surrounding soft tissue external to the IEE. This would be expected since RUNX2 is expressed in differentiating and mature osteoblasts and cementoblasts (Diep et al., 2009; and see Camilleri et al., 2006), contextually, since alveolar bone is already well established in the subadult hyrax, and since the RUNX2+ cells are close to cervical region and developing tooth roots, the reactive cells are most likely cementoblasts.

A somewhat surprising aspect of the replacement tooth germs is the lack of stellate reticulum in most premolars. As in the primary tooth germs, the stellate reticulum forms in replacement teeth at the beginning of the bell stage (Navarro et al., 1975). The function of the stellate reticulum is not completely clear, although it persistence throughout amelogenesis (Nanci, 2003) suggests a prolonged importance for the tooth germ. It was recently proposed that the stellate reticulum is a source of some cells within the papillary layer, a dental epithelial derivative that facilitates tooth eruption (Liu et al., 2016). The apparent lack of a stellate reticulum in P2, which is not yet erupting, may refute this idea, or may instead indicate alternative fate of the stellate reticulum in the hyrax.

4.3 Conclusion

In this study, a subadult hyrax with mixed dentition is examined histologically, the first detailed soft tissue study of a postnatal specimen. A notable histological characteristic of replacement premolars and the tusks is the expression of RUNX2, a marker that is expressed by ameloblasts at all stages of amelogenesis, in ameloblasts of the IEE.

Most premolars are pre-eruptive, but P4 exhibits evidence of ameloblasts still secreting protein; this tooth will not erupt for more than another year. In each of the premolars, the pulp chambers are relatively large compared to adults. This may indicate that the lengthy time in crypts is important for dentin production. The results also confirm that the hyrax has thin enamel on tusks, supporting the hypothesis that enamel is of limited importance for non-feeding behaviors.

REFERENCES

Adloff, P. (1903). Zur Kenntnis des Zahnsystems von Hyrax. Zeitschrift für Morphologie und Anthropologie, 5, 181–200.

Asher, R. J., Gunnell, G. F., Seiffert, E. R., Pattinson, D., Tabuce, R., Hautier, L., & Sallam, H. M. (2017). Dental eruption and growth in Hyracoidea (Mammalia, Afrotheria). *Journal of Vertebrate Paleontology*, *37*(3), e1317638.

Camilleri, S., & McDonald, F. (2006). Runx2 and dental development. *European journal of oral sciences*, *114*(5), 361-373.

Coady, J. M., Toto, P. D., & Santangelo, M. V. (1967). Histology of the mouse incisor. *Journal of Dental Research*, *46*(2), 384-388.

Diep, L., Matalova, E., Mitsiadis, T. A., & Tucker, A. S. (2009). Contribution of the tooth bud mesenchyme to alveolar bone. *Journal of Experimental Zoology Part B: Molecular and Developmental Evolution*, *312*(5), 510-517.

Deleon, V. B., & Smith, T. D. (2014). Mapping the nasal airways: using histology to enhance CT-based three-dimensional reconstruction in Nycticebus. *The Anatomical Record*, *297*(11), 2113-2120.

Fairall, N. (1980). Growth and age determination in the hyrax *Procavia capensis*. *African Zoology*, *15*(1), 16-21.

Fenton, M. B. (1992). Wounds and the origin of blood-feeding in bats. *Biological Journal of the Linnean Society*, *47*(2), 161-171.

Gomes Rodrigues, H., Tabuce, R., Asher, R. J., & Hautier, L. (2020). Developmental origins and homologies of the hyracoid dentition. *Evolution & development*, *22*(4), 323-335.

Hermanson, J. W., & Carter, G. G. (2020). Vampire bats. In: *Phyllostomid bats: A unique mammalian radiation*, pp 257-272.

Horne, W. A., & Loomis, M. R. (2007). Elephants and hyrax. Zoo Animal and Wildlife Immobilization and Anesthesia. Blackwell Publishing, Ames, IA, 507-521.

Kozawa, Y., Mishima, H., Suzuki, K., & Ferguson, M. W. J. (2001, October). Dental formula of elephant by the development of tooth germ. In *The World of Elephants: Rome, Proceedings of the First International Congress* (pp. 639-642).

Lee, J. H., Lee, D. S., Nam, H., Lee, G., Seo, B. M., Cho, Y. S., ... & Park, J. C. (2012). Dental follicle cells and cementoblasts induce apoptosis of ameloblast-lineage and Hertwig's

epithelial root sheath/epithelial rests of Malassez cells through the Fas–Fas ligand pathway. European Journal of Oral Sciences, 120(1), 29-37.

Legendre, L.F. (2002). Malocclusions in guinea pigs, chinchillas and rabbits. Can Vet J. 43, 385-90.

Liu, H., Yan, X., Pandya, M., Luan, X., & Diekwisch, T. G. (2016). Daughters of the enamel organ: development, fate, and function of the stratum intermedium, stellate reticulum, and outer enamel epithelium. *Stem cells and development*, *25*(20), 1580-1590.

Liu, X., Xu, C., Tian, Y., Sun, Y., Zhang, J., Bai, J., ... & Gao, Y. (2019). RUNX2 contributes to TGF-β1-induced expression of Wdr72 in ameloblasts during enamel mineralization. Biomedicine & Pharmacotherapy, 118, 109235.

Locke, M. (2008). Structure of ivory. *Journal of Morphology*, *269*(4), 423-450.

Luckett, W. P. (1993). An ontogenetic assessment of dental homologies in therian mammals. In *Mammal phylogeny: Mesozoic differentiation, multituberculates, monotremes, early therians, and marsupials* (pp. 182-204). New York, NY: Springer New York.

Moyano, S. R., Cassini, G. H., & Giannini, N. P. (2019). Skull ontogeny of the hyraxes *Procavia capensis* and *Dendrohyrax arboreus* (Procaviidae: Hyracoidea). *Journal of Mammalian Evolution*, *26*, 317-331.

Nasoori, A. (2020). Tusks, the extra-oral teeth. *Archives of Oral Biology*, *117*, 104835.

Navarro, J. A. C., SOTTOVIA-FILHO, D., Leite-Ribeiro, M. C., & Taga, R. (1975). Histological study on the postnatal development and sequence of eruption of the maxillary cheek-teeth of rabbits (Oryctolagus cuniculus). *Archivum histologicum japonicum*, *38*(1), 17-30.

Olds, N., & Shoshani, J. (1982). *Procavia capensis*. Mammalian Species, 171, 1-7.

Raubenheimer, E. J. (2000). Early development of the tush and the tusk of the African elephant (Loxodonta africana). *Archives of Oral Biology*, *45*(11), 983-986.

Sale, J. B. (1966). Daily food consumption and mode of ingestion in the hyrax. *J. East. Afr. Nat. Hist. Soc*, *25*, 215-224.

Steyn, D., & Hanks, J. (1983). Age determination and growth in the hyrax Procavia capensis (Mammalia: Procaviidae). *Journal of Zoology*, *201*(2), 247-257.

Towle, I., Salem, A. S., Veneziano, A., & Loch, C. (2023). Variation in enamel and dentine mineral concentration and density in primate molars. *Archives of Oral Biology*, *153*, 105752.

Virág, A. (2012). Histogenesis of the unique morphology of proboscidean ivory. *Journal of Morphology*, *273*(12), 1406-1423.

Whitney, M. R., Angielczyk, K. D., Peecook, B. R., & Sidor, C. A. (2021). The evolution of the synapsid tusk: insights from dicynodont therapsid tusk histology. Proceedings of the Royal Society B, 288(1961), 20211670.

Woodward, M. F. (1892). On the milk dentition of Procavia (Hyrax) capensis and of the rabbit (Lepus cunniculus), with remarks on the relation of the milk and permanent dentitions of the Mammalia. Proceedings of the Zoological Society of London, 38–49.

Wyss, F., Müller, J., Clauss, M., Kircher, P., Geyer, H., von Rechenberg, B., & Hatt, J. M. (2016). Measuring rabbit (Oryctolagus cuniculus) tooth growth and eruption by fluorescence markers and bur marks. *Journal of veterinary dentistry*, *33*(1), 39-46.

Figure legends

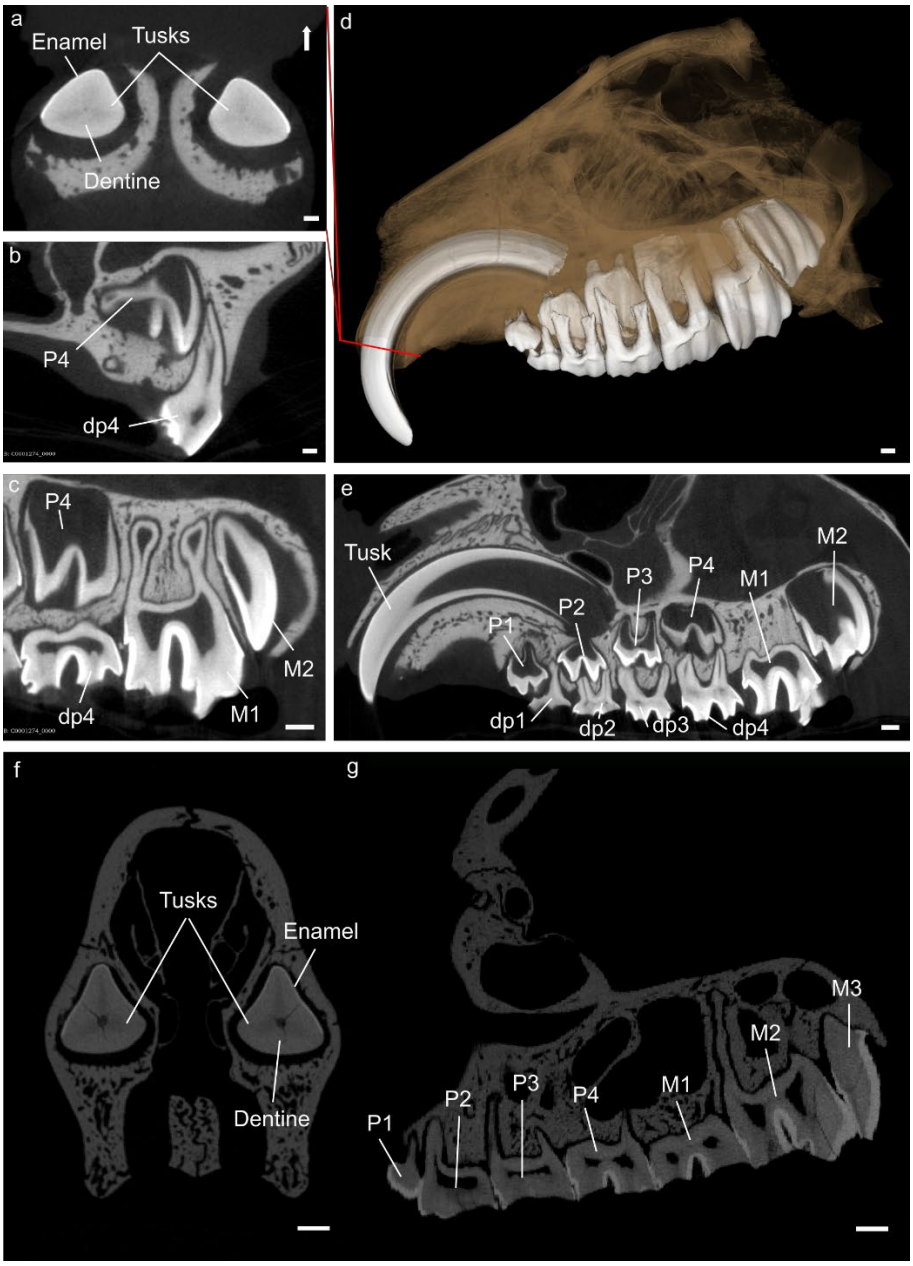

Figure 1: Three-dimensional reconstruction of the specimen M90628 (*Procavia capensis*). a- Cross-section of the tusks (incisors), the white arrow points toward the dorsal side. b- Coronal section of the dp4 and P4. c- Sagittal section of the dp4-P4 and M1-M2. d- Three-dimensional reconstruction of the specimen M90628 (Lateral view). e- Sagittal section of the left dental raw. f- Cross-section of the tusks of the adult specimen H5101A. g- Sagittal section of the dental row (same specimen as 5). In all sagittal view, left side = rostral. Scale=1mm.

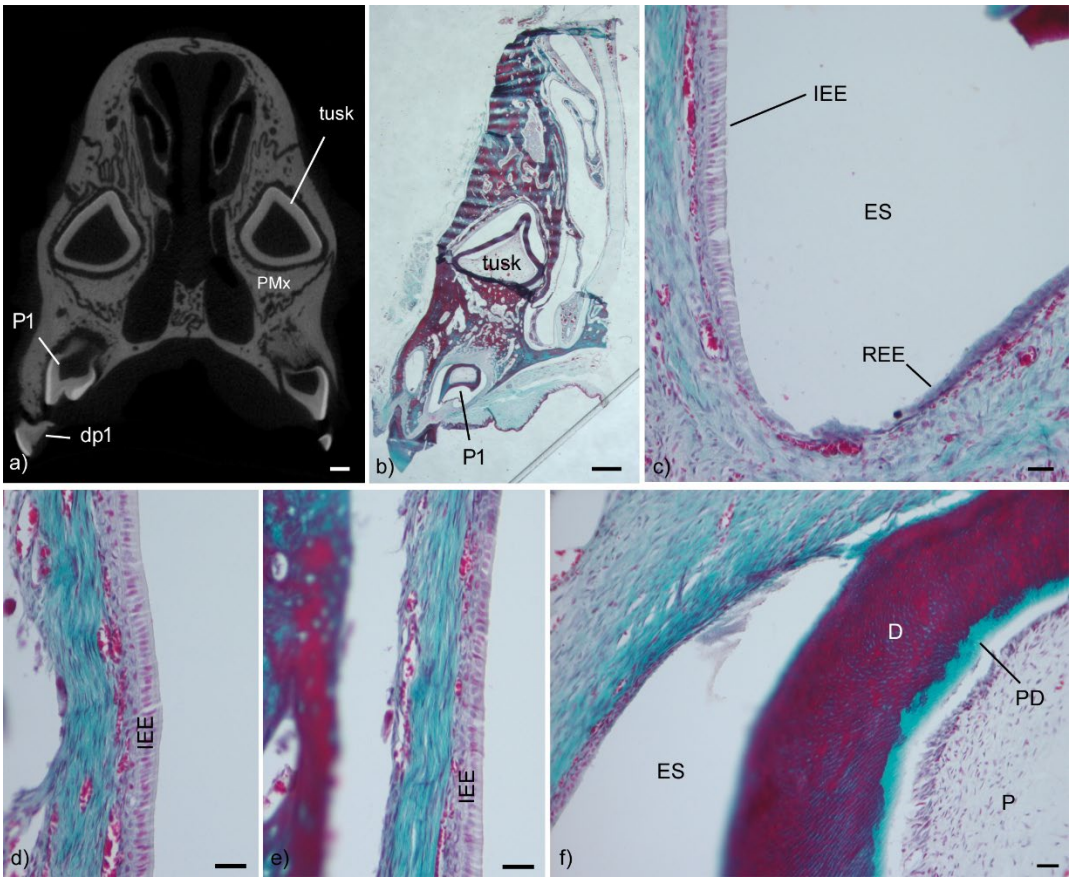

Figure 2: The tusk (I1) and first deciduous (dp1) and replacement premolar (P1) in the subadult hyrax. The tusk housed within the premaxilla (PMx) at the same level as the first premolar are shown in microcyte (a) and histology (b). c) P1 has inner enamel epithelium (IEE) adjacent to the enamel space (ES) on buccal and lingual sides, whereas the occlusal side is covered by reduced enamel epithelium (REE). d, e) The IEE is high columnar epithelium along much of the crown, diminishing in height near the cervical region. f) The dentin (D) stains deeply red with Gomori trichrome stain, as contrasted with bright green predentin (PD). Scale bars: a, b, 1 mm; c-f, 30 µm.

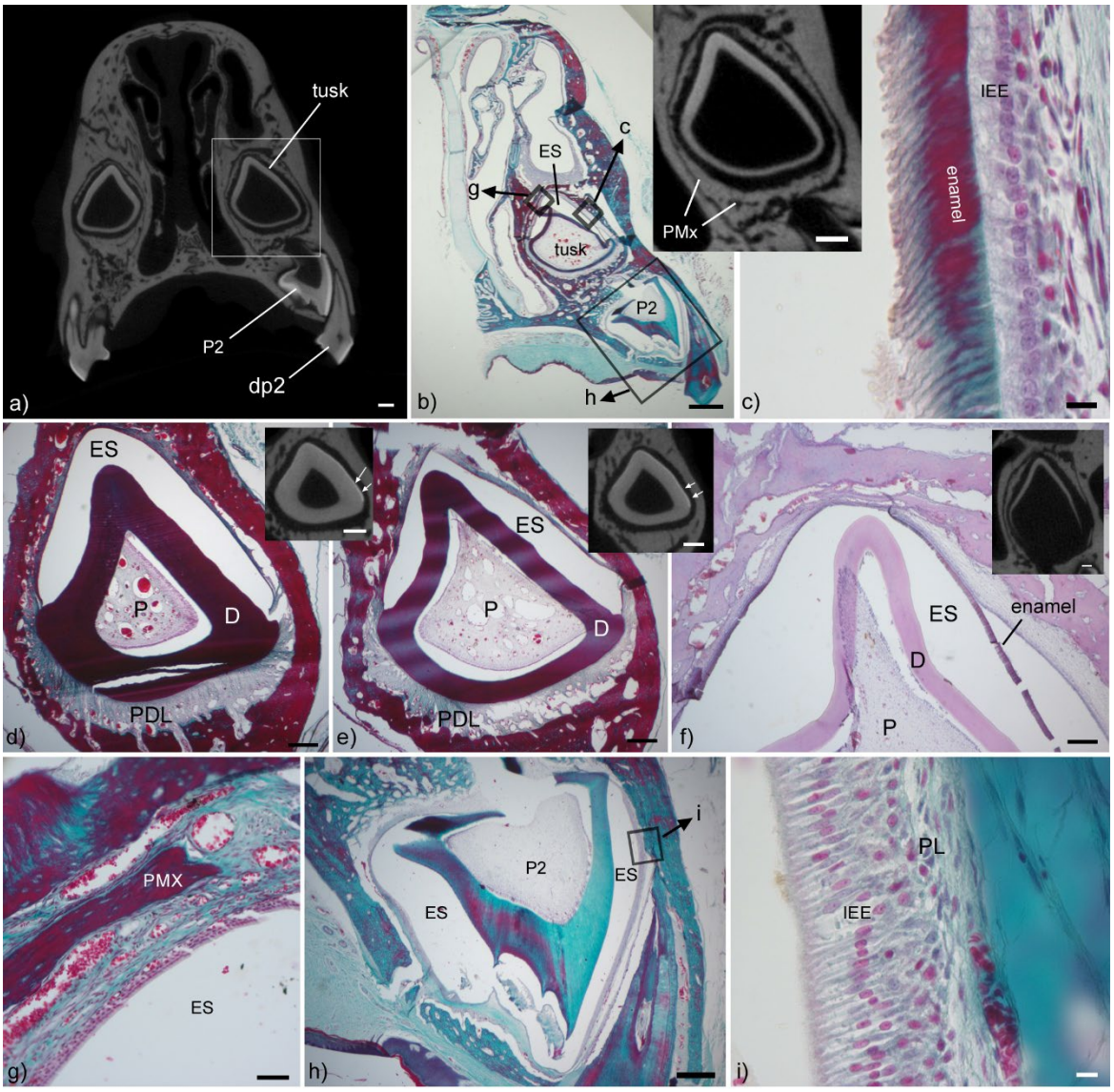

Figure 3: The tusk (I1) and second deciduous (dp2) and replacement premolar (P2) in the subadult hyrax. The tusk housed within the premaxilla (PMx) at the same level as the first premolar are shown in microCT (a) and histology (b). c) magnified view of the tusk crypt (see box in b for location), showing the internal enamel epithelium (IEE) and a thin fragment of enamel. E-f) rostral to caudal series of the tusk; e is rostral to the premolar, and f is at the same level as P3/dp3. Note the greatly increased dentin thickness from caudal to rostral; thin enamel is detectable caudally (f), whereas an enamel space (ES) is observed at more rostral levels. G) The wall of the tusk crypt caudally (see box in b for location), showing a thin shell of the PMx. h) Low magnification view of P2, showing thick dentin and an ES to its lingual and buccal sides. A box indicates the location of the enlarged view in i, which reveals the high columnar IEE. PL, papillary layer. Scale bars: a, b, 1 mm; c, 10 µm; d, e, 400 µm ; f, 200 µm; g, 50 µm; h, 0.5 mm; I, 10µm; all insets, 1 mm.

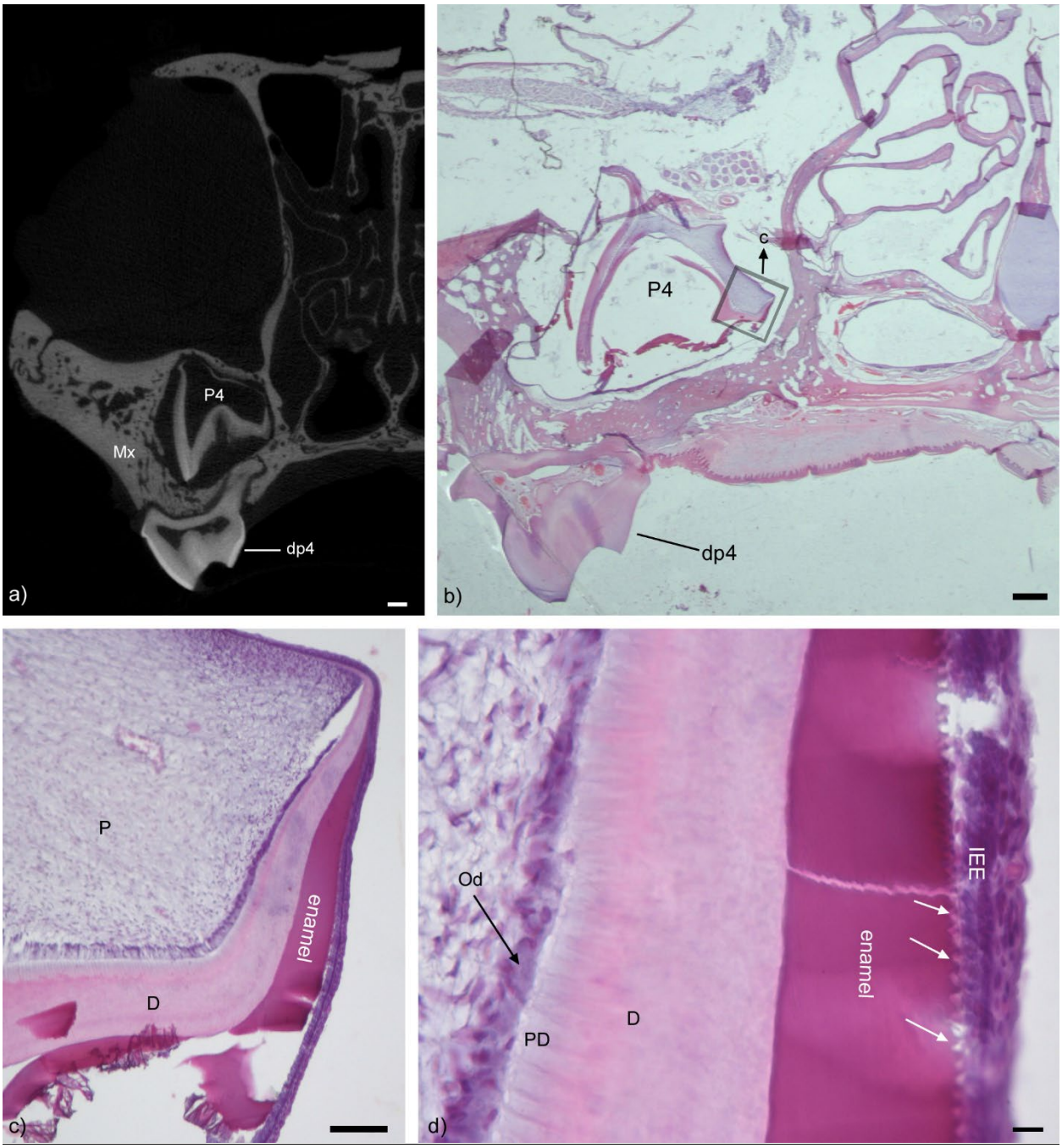

Fig. 4: The fourth deciduous (dp4) and replacement premolar (P4) in the subadult hyrax, shown in microCT (a) and histology (b). The boxed region in b is enlarged in c, revealing part of the pulp cavity (P) and adjacent dentin (D) and enamel. The enamel is fragmentary near the occlusal side of the crown. But closer to the cervix (d, showing an adjacent section) the enamel is intact. The internal enamel epithelium has a "picket-fence" appearance (white arrows), indicating the presence of Tomes' processes at the apex of the ameloblasts. Scale bars: a, 1 mm; b, 0.5 mm; c, 100 µm; d, 10 µm.

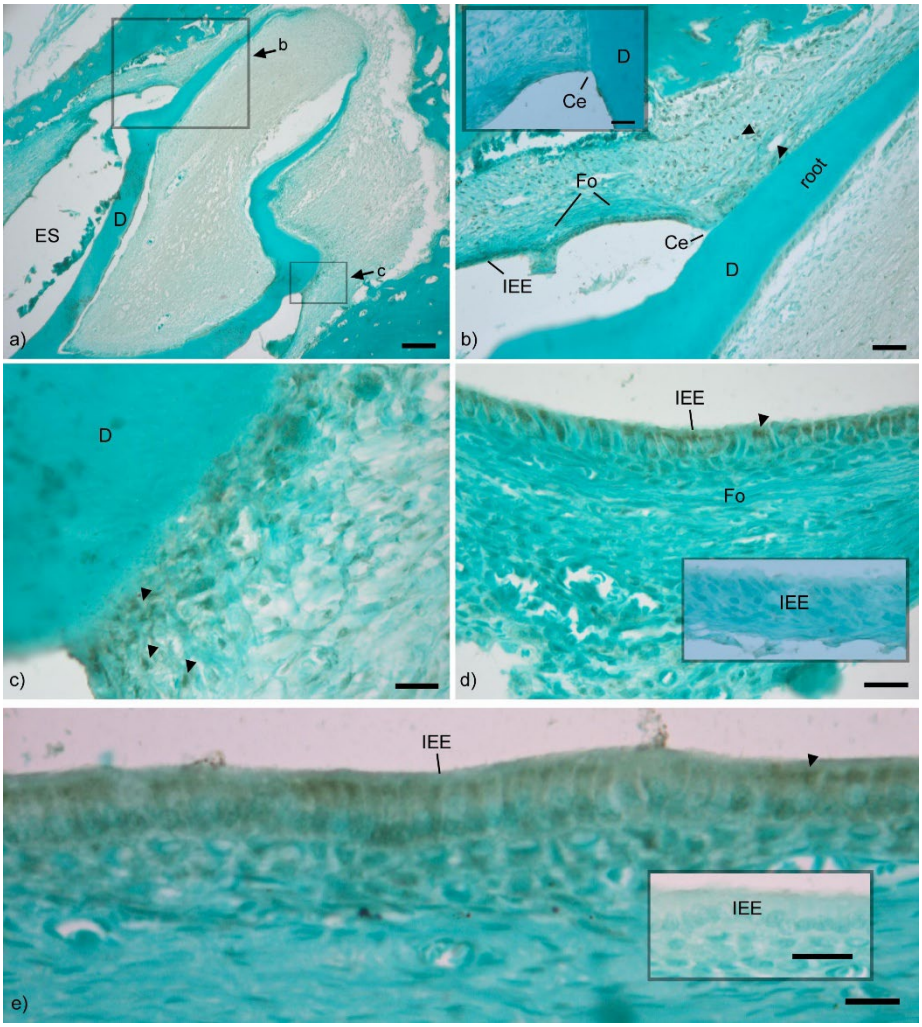

Figure 5: A section prepared using RUNX2 immunohistochemistry (fast green counter stain), showing the replacement premolar (P1) in the subadult hyrax. a) This section shows the root (upper right) and part of the crown, excluding the enamel, which was destroyed during the decalcification process. b) An enlargement of the cervical (Ce) region of the same tooth reveals few reactive cells near the crown, but sparse moderately RUNX2+ cells (arrowheads) are present adjacent to the root. c) High magnification view of the cervical region (see box in plate a for location), showing RUNX2+ cells near the cervical region. d) The internal enamel epithelium (IEE) of the same tooth, but more apical to the field of view in plate a. The IEE has numerous RUNX2+ ameloblasts. Note there are no RUNX2+ below the heavily fibrous inner layer of the follicle (Fo). E) The IEE also has numerous RUNX2+ ameloblasts. Insets in b, d and e show there is no discernable non-specific background staining in negative controls. Scale bars: a, 200 μm; b, 50 μm; c, d, e and all insets, 20 μm.